**Pharmacological fatty acid synthase inhibitors differently affect the malignant phenotype of oral cancer cells**

Willian Peter Boelcke [a,b,1], Isadora Ferrari Teixeira [b,1], Iara Gonçalves Aquino [b], Amanda Ramos Mazzaro [a], Florence Juana Maria Cuadra-Zelaya [b,c], Ana Paula de Souza [a], Tuula Salo [d,e], Ricardo Della Coletta [b], Edgard Graner [b], D´ebora Campanella Bastos [a,b,*]

[a] Department of Biociences, School of Dentistry, University of Campinas, Piracicaba, SP, Brazil

[b] Department of Oral Diagnosis, School of Dentistry, University of Campinas, Piracicaba, SP, Brazil

[c] Department of Pathology, University of El Salvador, San Salvador, El Salvador

[d] Cancer and Translational Medicine Research Unit, Faculty of Medicine and Medical Research Center Oulu, Oulu University Hospital, University of Oulu, Oulu, Finland

[e] Institute of Oral and Maxillofacial Disease, University of Helsinki, and HUSLAB, Department of Pathology, Helsinki University Hospital, Helsinki, Finland

* Correspondence to: Department of Biosciences, School of Dentistry of Piracicaba, State University of Campinas (UNICAMP), Av. Limeira 901, Are˜ao, Piracicaba

13414-018, S˜ao Paulo, Brazil.

E-mail address: bastosdc@unicamp.br (D.C. Bastos).

[1] These authors contributed equally to this work.

Keywords: Fatty acid synthase, FASN inhibitors, Oral cancer

## ABSTRACT

Objective: Fatty acid synthase levels are associated with aggressiveness, prognosis, and risk of metastasis in oral squamous cell carcinomas. This enzyme contains seven catalytic domains and its inhibition by synthetic or natural drugs has antineoplastic properties such as C75, which is a synthetic inhibitor of the β- ketoacyl synthase domain, the antibiotic triclosan, ligand of the enoyl reductase domain, and the antiobesity drug orlistat, which inhibits the thioesterase domain. Here, we sought to investigate and compare the in vitro effects of C75, triclosan, and orlistat on malignant phenotypes of the cell line SCC-9: proliferation, cell cycle, apoptosis, adhesion, migration, and invasion.

Design: Half-maximal inhibitory concentration (IC50) was determined using cell viability assays. Cell death and cell cycle progression were analyzed by Annexin V-PE/7-ADD-PerCP labeling and propidium iodide staining, respectively. Cell migration and invasion were assayed by transwells assays and cell adhesion using collagen and fibronectin.

Results: C75 showed the lowest $IC_{50}$ and higher inhibition of lipid droplets at low concentrations and reduced cell motility. Triclosan showed the intermediate $IC_{50}$ value, excellent reduction of lipid bodies at the $IC_{50}$ when compared with C75 and orlistat. Also, triclosan reduced cell cycle progression, adhesion, migration, and invasion of SCC-9 and induced the highest levels of apoptosis. Orlistat promoted cell cycle arrest, but showed the lowest induction of apoptosis and did not affected invasion and adhesion of SCC-9.

Conclusion: Altogether, despite the particular effects of the analyzed fatty acid synthase inhibitors, triclosan showed to better interfere in tumorigenic phenotypes of SCC-9 cells.

## INTRODUCTION

Head and neck cancer is the sixth most common cancer worldwide and annually accounts more than 650,000 cases and 330,000 deaths (Bray et al., 2018). More than 90% of all types of head and neck cancers are squamous cell carcinomas that affect the oral mucosa (Montero & Patel, 2015). Clinically, oral squamous cell carcinoma (OSCC) shows a locally aggressive behavior, frequent recurrences, and regional or distant metastases (Ho et al., 2017). Despite the efforts and new modalities of treatments, the mortality rates of OSCC remain unchanged for decades, with a 5-year survival rate of around 50% (Cohen Goldemberg, de Araújo, Antunes, de Melo, & Santos Thuler, 2018).

The reprogramming of energy metabolism plays an important role in carcinogenesis and has been included as a hallmark of cancer by providing metabolic targets for cancer treatment (Hanahan & Weinberg, 2011). Accordingly, several studies demonstrate an aberrant expression of the enzyme fatty acid synthase (FASN) and increased endogenous lipogenesis in several human cancers and its precursors, including OSCC (Angeles & Hudkins, 2016; Menendez & Javier A, 2017; Menendez J.A, 2017; Silva et al., 2008, 2009, 2010). FASN is the multi-enzyme protein responsible for the de novo biosynthesis of long-chain fatty acids, especially palmitate, from acetyl-CoA and malonyl-CoA (Angeles & Hudkins,2016; Kuhajda, 2000). Structurally, FASN is formed by two polypeptide chains (~270 kDa) containing seven different catalytic domains sequentially organized from the N-terminal to the C-terminal: β-ketoacyl synthase, acetyl-CoA transacylases and malonyl-CoA transacylases, dehydratase, enoyl reductase, β-ketoacyl reductase, and thioesterase site and the acyl carrier protein (Menendez & Javier A, 2017; Menendez J.A, 2017; Smith, Witkowski, & Joshi, 2003).

Under normal conditions, FASN levels in human tissues are usually low, since the cells utilize circulating lipids mainly from the diet (Menendez et al., 2004). In contrast, cancer cells highly express FASN to fuel membrane production, lipid-based post-translational protein modifications, redox balance maintenance, and energy metabolism (Menendez & Javier A, 2017; Menendez J.A, 2017; R¨ohrig & Schulze, 2016). In OSCC, FASN is overexpressed, associated with overall survival rates, and with the histological grade, lymphatic permeation, perineuralinfiltration, and lymph node metastasis (Silva et al., 2008, 2009).

In the last decade, several natural or synthetic FASN inhibitors have been described to promote anticancer effects by interfering in the lipogenic dependency (Angeles & Hudkins, 2016; Buckley et al., 2017; Chu, Deng, Man, & Qu, 2017; Menendez & Javier A, 2017; Menendez J.A, 2017). Among the most studied are cerulenin, and its synthetic derivative C75, the antibiotic triclosan (TCS) and orlistat (ORL), a drug approved by FDA for the treatment of obesity (Liu, 2006; Lupu & Menendez,

2006; Rendina & Cheng, 2005; Wang et al., 2009). Cerulenin and C75 interact with the β-ketoacyl synthase domain and irreversibly inhibit the condensation reaction and (Rendina & Cheng, 2005). TCS blocks FASN activity through hydrogen bonding and hydrophobic interactions with specific amino acids in the enoyl reductase domain (Liu, Wang, Fillgrove, & Anderson, 2002; Menendez & Javier A, 2017; Menendez J.A, 2017). On the other hand, ORL inhibits FASN activity through a covalent adduct with the thioesterase domain (Kridel, Axelrod, Rozenkrantz, & Smith, 2004; Menendez & Javier A, 2017; Menendez J.A, 2017).

Importantly, pharmacological or genetic inhibition of FASN selectively induces cancer cell death and reduction of tumor progression in mouse models (Angeles & Hudkins, 2016; Jones & Infante, 2015; Menendez & Javier A, 2017; Menendez J.A, 2017). Besides the classical FASN inhibitors, next-generation drugs have shown significant effects with high selectivity. IPI-9119, a specific non-commercial inhibitor of the thioesterase domain of FASN, is able to reduce the growth of prostate cancer xenografts and human organoids by inducing substantial metabolic reprogramming (Zadra, 2019). TVB-3166 is an imidazopyridine-based molecule which inhibits the β-ketoacyl reductase domain, reduces proliferation of several cancer cell lines by interfering in oncogenic pathways, especially PI3K-AKT-mTOR and β-catenin, and, when combined with paclitaxel, decreases the growth of the prostate xenografts (Heuer et al., 2017; Oslob et al., 2013; Ventura et al., 2015). Our group recently demonstrated that TVB-3166 decreases the viability and migration and induces apoptosis and cell cycle arrest of OSCC (Aquino et al., 2020). Moreover, TVB-2640 (ASC40), an analogue of TVB-3166, is the first FASN inhibitor included in clinical trials for patients with solid tumors (NCT02223247), as well as in phase II trials for colon (NCT02980029), KRAS mutated non-small cell lung carcinomas (NCT03808558), astrocytomas (NCT03032484), ErbB2 positive breast cancer (NCT03179904) and glioblastomas (NCT05118776). Finally, Omeprazole, an inhibitor of proton pump, was recently reported to inhibit FASN in gastric epithelial cells (Chen et al., 2020) and was safety when administrated for patients with triple negative breast cancer in dosis that inhibited FASN (Sardesai et al., 2021). In fact, clinical trials aiming to evaluate the response of this drug in castration resistant prostate cancer and breast cancer are also being conducted (NCT04337580; NCT02595372).

Here we describe for the first time the effects of the pharmacological inhibition of distinct catalytic domains of FASN with C75, TCS, and ORL in SCC-9 cells.

## MATERIALS AND METHODS

## 2.1. Cell culture

Human OSCC (SCC-9) cells (American Type Culture Collection–ATCC, Manassas, VA, USA) were originally isolated from a tongue squamous cell carcinoma of a 25 years-old male and its tumorigenic phenotype is well documented in the literature by ours and other groups (Agostini et al., 2014; de Andrade, Rodrigues, Rodini, & Nunes, 2017; Liu et al., 2002; Ramos et al., 2002; Rheinwald & Beckett, 1981). SCC-9 were cultured in DMEM/F-12 medium (Invitrogen, Carlsbad, CA, USA) supplemented with 2% or 10% FBS (Cultilab, Campinas, Brazil), 400 ng/mL hydrocortisone (hydrocortisone sodium succinate - Eurofarma, Brazil) and 1:100 antibiotic/antimycotic solution (Invitrogen) at 37 ◦C in a humidified atmosphere containing 5% CO2. C75, TCS, ORL, and the vehicle DMSO (Dimethylsulfoxide, Sigma, St Louis, MO, USA) were added to the culture medium at the concentrations described in Table 1.

## 2.2. Proliferation assay and calculation of the $IC_{50}$

Cell viability was determined by seeding 8 × 104 SCC-9 cells in 12-well plates with DMEM/F-12 containing 10% FBS. After 24 h, cells were, serum-starved for additional 24 h for cell cycle synchronization. After, the medium was replaced by 500 μL of DMEM/F-12 supplemented with 2% FBS containing increasing concentrations of C75, TCS or ORL (Sigma) for 24 or 48 h. The volume of the vehicle DMSO was adjusted for each concentration. Control cells were treated with the maximum volume of DMSO. Cell viability was determined after the incubation with 25 mg/mL of MTT (4,5-dimethylthiazol-2-yl) 25 mg/mL of MTT (4,5-dimethylthiazol-2-yl) − 2,5 diphenyltetrazolium bromide (Sigma) for 4 h. After this period, formazan crystals produced by viable cells were eluted in absolute ethanol and the absorbance was determined with the aid of a microplate reader (Bio-Rad, Hercules, CA, USA) at 550 nM and corrected at 650 nM. Inhibitory concentration 50% ($IC_{50}$) values were calculated by the dose-effect curve using the CompuSyn software (Cambridge, MA, USA) as previously described (Chou & Martin, 2005).

## 2.3. Bodipy staining for lipid droplets

In order to confirm the FASN inhibition by C75, TCS, and ORL, we performed BODIPY™ (Invitrogen) staining for neutral lipids by plating 2 × 103 SCC-9 cells in each well of 8-well chamber slides (Lab-tek, Thermofisher-Nunc). After 24 h, the medium was replaced by 500 μL of DMEM-F12 without FBS and, following additional 24 h, cells were incubated with the concentrations

corresponding to the IC12.5, IC25, and IC50 of the studied drugs diluted in DMEM/F12 with 2% FBS for 24 and 48 h. After this period, lipid droplets were stained by adding 3.8 µM of bodipy in the cell media (DMEMF/12 with 2% FBS) for 1 h at 37 °C. Cells were washed with PBS, fixed with absolute formaldehyde with 10% CaCl2 for 30 min, washed again, and the slides mounted in aqueous media. At least 10 micrographies for each condition were captured and analyzed in an epifluorescence microscope (Leica DMR, Wetzlar, Germany). The number of lipid bodies was counted and normalized by the corresponding cell area with the aid of the Image J software (National Institute of Health, Bethesda, Maryland, USA).

### 2.4. Cell cycle and apoptosis analysis

For the flow cytometry analyses, cells were plated in 25 cm2 culture flasks, serum-starved for 24 h, and treated for 48 h with three different concentrations of the FASN inhibitors. Cells were then harvested by trypsinization and centrifuged at 900xg. To determine SCC-9 distribution in each phase of the cell cycle, cells were fixed in cold 70% ethanol for at least 16 h at − 20 °C, and, after washing in cold PBS treated with 10 µg/mL RNAse (Sigma) at 37 °C for 1 h and incubated with 50 µg/mL propidium iodide at 4 °C for 2 h. To determine the percentage of apoptotic and necrotic cells, cells were washed in PBS and incubated with Annexin V-FITC (1:100) and 7-AADPerCP (1:200) in a binding buffer containing 10 mM HEPES (pH 7.4), 150 mM NaCl, 5 mM KCl, 1 mM MgCl 2 and 1.8 mM CaCl2 in the dark for 20 min at room temperature. Ten thousand events were acquired, analyzed by flow cytometry on FL-1 or FL-2 channel of a FACS Calibur (BD Biosciences, San Jose, CA, USA) equipped with an argon laser for apoptosis and cell cycle respectively. The distribution of cells in the cycle was evaluated with the software ModFit (Verity Software House) and the percentage of apoptotic or necrotic cells calculated by the software CellQuest (Becton Dickinson and Company, San Jose, CA, USA).

### 2.5. Cell adhesion assays

Four wells of a 96 well plate were sensitized with 10 µg/cm2 of type I collagen or fibronectin diluted in 100 µL of PBS and as, negative controls, with 100 µL of PBS. The plates were maintained for 24 h at 4 °C and, after this period, each well was washed with PBS and blocked with 200 µL 3% BSA for 2 h at 37 °C. After the treatment with FASN inhibitors for 48 h, cells were trypsinized and resuspended in DMEM/F12 supplemented with 3% BSA. For each condition, 3 × 104 cells diluted in

100 µL of DMEM/F12 supplemented with 3% BSA were plated in each well of the previously sensitized plates and incubated for 45 min to 1 h. The period of adhesion was determined by observation in a phase contrast microscope. Non-adherent cells were washed 3 times with 100 µL of PBS and the adherent cells fixed with 4% formalin for 15 min at room temperature. Cells were then stained with an aqueous solution of 1% toluidine blue and 1% borax for 5 min. The excess of dye was removed by vigorous washing in distilled water. After elution in 100 µL of a 1% SDS, the absorbances were determined at 655 nM in a microplate reader (Bio-Rad, Hercules, CA, USA).

### 2.6. Transwell migration and invasion assays

The effects of C75, TCS, and ORL in the migratory phenotype of SCC-9 cells were evaluated by transwell migration assays. Prior to the plating, cells were serum-starved for 24 h and treated with the IC50 of C75, TCS, or ORL for additional 24 h. Briefly, 8 × 104 SCC-9 cells were resuspended in 200 µL of FBS-free DMEM/ F-12 and added in the upper compartment of each 8 µM pore Transwell™ nylon filter membrane insert. In the lower compartment of each transwell were added 1 mL of DMEM/F-12 containing 2% FBS and FASN inhibitors or vehicle. After 24 h, migrating cells were fixed in 10% formalin for 10 min and stained by 1% toluidine blue. The inserts were washed with distilled water and the cells of the upper compartment carefully removed with distilled water-soaked cotton swabs. After elution with 500 µL of 1% SDS, the absorbances were read at 655 nM in a microplate reader (Bio-Rad). Invasion assays were performed as previously described (Mendonça et al., 2017, Salo et al., 2015). First, 60 µL of a 3.22 µg/mL myogel solution were added in the upper chamber of 8-µM pore Transwell™ inserts and solidified at 37 °C for 30 min. After this period, serum-starved SCC-9 cells (3 ×105 for each condition) were resuspended in serum-free medium containing the IC50 concentrations of each FASN inhibitor or DMSO and seeded onto the insert with solidified myogel. The lower compartments of the transwells were filled with 1 mL of DMEM/F-12 supplemented with 2% FBS and the respective FASN inhibitors or the vehicle. After 48 h, invasive cells were fixed with 10% formalin for 10 min and stained with 1% toluidine blue for 1 h at room temperature. After washing the non-adherent cells and elution with 500 µL of 1% SDS, the absorbances were read at 650 nM in a microplate reader (Bio-Rad).

### 2.7. Statistical analysis

All experiments were performed in technical replicates and repeated at least three times independently. The appropriate statistical tests were applied according to the data distribution. Normal distribution was verified using Shapiro-Wilk or D'Agostino-Pearson (Bodipy quantification) tests and comparisons between groups were performed using one-way ANOVA with Tukey's post-hoc analysis. The significance level was 95% ($p < 0.05$).

## RESULTS

### 3.1. C75, TCS, and ORL reduce SCC-9 proliferation and induce distinct morphologic changes

The IC50 for each drug (Table 1) was calculated based on the amount of viable cells by using dose-response curves with MTT assays (Fig. 1). Cell death was measured by the treatment with increasing concentrations of C75, TCS, and ORL for 24 h (Fig. 1A-C) or 48 h (Fig. 1D-F) and, as expected, we observed a dose-dependent effect in all analyzed conditions. C75 reduced the SCC-9 viability in a dose-dependent manner in 24 h (Fig. 1 A) and 48 h (Fig. 1D) in concentrations lower than 30 µM. On the other hand, TCS was not effective in SCC-9 cells in lower concentrations but highly affected the SCC-9 viability in concentrations above 36 µM for 24 h (Fig. 1B) and 18 µM for 48 h (Fig. 1E). ORL reduced SCC-9 viability in concentrations higher than 100 µM for 24 h (Fig. 1 C) and 50 µM for 48 h (Fig. 1 F). The morphology of SCC-9 treated with C75, TCS, or ORL for 24 h (Fig. 1 G-J) or 48 h (data not shown) was monitored using phase contrast microscopy and compared with DMSO treated cells. Each drug promoted distinct morphologic changes in SCC-9 cells, however, the morphology was not affected by the period of treatment (24 or 48 h). As seen in Fig. 1G, SCC-9 cells incubated with the vehicle showed an accentuated pleomorphism with the predominance of polygonal shaped cells, large nuclei, and evident nucleoli. The treatment with C75 promoted an evident cytoplasmatic enlargement and a decrease of the nucleus/cytoplasm ratio (Fig. 1H, arrows). SCC-9 cells treated with TCS showed an important reduction in cell size and an increase of cytoplasmic granules (Fig. 1I, arrows). Finally, treatment with ORL promoted an evident cytoplasmic retraction and cell elongation compared to the control group (Fig. 1J). All compounds increased the number of detached rounded cells characteristic of dead cells (Fig. 1H-J, arrowheads).

### 3.2. FASN inhibition reduce lipid droplets in SCC-9 cells

In order to confirm that the effects of C75, TCS, and ORL on SCC-9 cells are associated with the reduction of FASN activity, we used bodipy to stain intracellular lipid droplets. These studies showed

that, compared to the vehicle (Figs. 2A and S1A), all the concentrations of C75 reduced the lipids droplets of SCC-9 cells in 24 h (Fig. S1) and 48 h (Fig. 2), and the concentration corresponding to its $IC_{50}$ had the highest effect on FASN inactivation in 24 h (83% of inhibition, Fig. S1B, E). Similar effects were found by treating SCC9 cells with C75 for 48 h (Fig. 2A-E). On the other hand, TCS showed a dose-dependent effect and maximum FASN inhibition with the dose relative to the $IC_{50}$ when SCC9 were treated for 24 h (95% of lipid droplets reduction, Figs. S1C, F). Similar results were obtained when the cells were treated for 48 h (Fig. 2F-J). ORL was the less effective and reduced 28% and 38% of lipid bodies in SCC-9 cells treated with its $IC_{25}$ and $IC_{50}$ for 24 h, respectively (Figs. S1D, G). We also did not observed statistical differences when SCC9 were treated with the IC12.5 of ORL for 48 h (Fig. 2O). However, the treatment with the $IC_{25}$ and the $IC_{50}$ of ORL for 48 h of significantly reduced the lipid bodies of SCC9 cells (Fig. 2K-O).

### 3.3. C75, TCS and ORL induces cell cycle arrest and apoptosis in SCC-9 cells

In order to better characterize the effects of FASN inhibitors on SCC-9 cells, we next performed cell cycle and apoptosis analysis by flow cytometry. The treatment with different concentrations of C75 (Fig. 3A), TCS (Fig. 3B), and ORL (Fig. 3C) for 48 h resulted in the accumulation of cells in the G0/G1 phase and significant reduction of the S phase. The number of cells in the G2/M phases of the cell cycle was not affected by the studied drugs (Fig. 3A-C). The $IC_{50}$ of C75 increased in 23.19% the number of cells in G0/G1 (Control: 45.05%; C75 $IC_{50}$: 68.25%) and reduced in 17.62% the number of cells in the S phase (Control: 35.04%; C75 $IC_{50}$: 17.42%). The IC50 of TCS resulted in an accumulation of cells in G0/G1 of 35.81% (Control: 49.05%; TCS $IC_{50}$: 84.86%) while the S phase was reduced in 26.8% (Control: 32.39%; TCS $IC_{50}$: 5.59%). Finally, cells in G0/G1 were increased by ORL in 31.58% (Control: 52.08%; ORL $IC_{50}$: 83.67%) and the S phase reduced in 24.05% (Control: 29.82; ORL $IC_{50}$: 5.77%). To compare the effects of the studied drugs on proliferating SCC-9 cells, we performed statistical analyzes with the number of cells in S phase (Fig. 3D-F) and found that TCS and ORL similarly affected cell cycle progression.

75 (Fig. 4A), TCS (Fig. 4B), and ORL (Fig. 4C) significantly reduce the number of viable cells and increase the number of apoptotic cells in a dose-dependent manner. As expected, the highest effect was observed in the concentration relative to the $IC_{50}$, in which $C_{75}$ (Fig. 4 A) and ORL (Fig. 4 C) increased the apoptotic levels in 5.5X and 4.58X, respectively (Control: 1.63; C75: 8.94 and Control: 1.13; ORL: 5.17). TCS showed the highest effect with an increase of the apoptotic cells in 21.89X (Control: 1.08; TCS $IC_{50}$: 21.89) (Fig. 4B). At low concentrations, TCS was also effective promoting

a dose dependent increase in apoptotic levels (1.75X for the IC12.5 and 8.42X for the $IC_{25}$). Statistical analysis comparing the effects of the drugs using the concentration relative to the $IC_{50}$ showed that TCS was the most effective drug in reducing the number of live cells (Fig. 4D) and increasing the percentage of apoptotic cells (Fig. 4E). Necrosis was not significantly affected by the drugs. Gate information were provided in the Figs. S2 (cell cycle) and S3 (apoptosis).

### 3.4. Adhesion, migration, and invasion of SCC-9 cells were differently affected by C75, TCS, and ORL

In order to verify the effects of C75, TCS, and ORL on the adhesion of SCC-9 cells to extracellular matrix components, cells were treated for 48 h with different concentrations of the drugs and allowed to adhere in previously sensitized plates with fibronectin or type I collagen. These studies showed a slight increase, not statistically significant, in the adhesion of SCC-9 cells treated with the IC12.5. No significant reduction in the cell adhesion to the matrix components was observed in the IC25 and IC50 concentrations of C75 (Fig. 5A). The adhesion of SCC-9 cells was significantly reduced with TCS in a dose-dependent manner (Fig. 5B) while ORL did not affect the adhesion to both type I collagen and fibronectin (Fig. 5C).

By using transwell cell migration (Fig. 6A-D) and invasion (Fig. 6F-I) assays, we observed that the treatment with the IC50 of C75, TCS, and ORL for 48 h reduced in 56%, 65.7%, and 31% the migration of SCC-9 cells, respectively (Fig. 6E). The invasive ability of SCC-9 cells were similarly reduced by C75 and TCS and not modified by ORL, when compared with the control cells (Fig. 6J).

## DISCUSSION

FASN is the key enzyme of the endogenous lipid metabolism and its activity is associated with signaling pathways and maintenance of the structure and function of cancer cell membranes (Buckley et al., 2017). Upregulation of FASN was demonstrated in several human malignancies, including oral cancer (Agostini et al., 2014, Aquino et al., 2020, Kelber et al., 2010, Ricklefs et al., 2020, Sadowski et al., 2014, Sippel et al., 2014). FASN has emerged as a therapeutic target due to its differential expression in normal and malignant tissues and its association with survival rates and prognosis (Röhrig and Schulze, 2016, Witkiewicz et al., 2008). Importantly, the multiple catalytic domains of FASN allowed the development of several FASN inhibitors through the last decade (Röhrig & Schulze, 2016). The first generation of FASN inhibitors provided the basis for the development and

testing of new FASN-targeted drugs and clarifying the role of FASN and lipid metabolism in cancer cells (Menendez and Lupu, 2017b, Menendez and Lupu, 2017a). Classic FASN inhibitors, such as C75, TCS (triclosan), and ORL (orlistat), were reported to promote cell death in vitro and in vivo in several types of cancer cells, including OSCC (Agostini et al., 2014, Bastos et al., 2017, Menendez and Lupu, 2017b, Menendez and Lupu, 2017a, Zadra and Loda, 2019).

SCC-9, a model of OSCC shows a tumorigenic phenotype, documented in the literature by ours and other groups (Agostini et al., 2014, de Andrade et al., 2017, Liu et al., 2002, Ramos et al., 2002, Rheinwald and Beckett, 1981) . Here, we demonstrated that ORL has the highest IC50 when compared with C75 and TCS. Our group has previously shown the anti-tumoral effects of ORL in melanoma (Bastos et al., 2017, Carvalho et al., 2008, Seguin et al., 2012) and OSCC cells lines (Agostini et al., 2014) by using similarly high concentrations. On the other hand, a 50% reduction of the SCC-9 viability was found at smaller concentrations of C75 and TCS in both, 24 h and 48 h. There is no data in the literature regarding the effects of C75 and TCS in oral cancer cells. Though, our IC50 concentrations for C75 were similar to the results of previous studies in cells lines derived from breast, lung, and prostate cancers (Chen et al., 2012, Giró-Perafita et al., 2016, Menendez et al., 2016, Puig et al., 2008, Relat et al., 2012, Sadowski et al., 2014). Also, the IC50 for TCS in retinoblastoma cells is 60 μM and between 4.5 and 6.9 μM in different prostate cancer cell lines (Deepa et al., 2012, Sadowski et al., 2014, Vandhana et al., 2013).

In our work, C75 reduced lipid droplets similarly at lower and higher TCS showed a dose-dependent reduction in lipogenesis. ORL also reduced the lipid bodies at its IC25 and IC50. Despite their distinct rates of FASN inhibition, all drugs reduced the S phase and increased the number of SCC-9 cells in the G0/G1 phases. Accordingly, several studies have demonstrated that FASN inhibitors promote a cell cycle arrest in several human cancer cell lines (Veigel et al., 2015). Agostini et al. (2014) demonstrated that the S phase of SCC-9 cells treated with ORL extracted from Orlistate (NeoQuímica Farmacêutica, Brazil) capsules for 72 h was reduced by approximately 75%. Similarly, Aquino et al. (2020) showed that TVB-3166, a new imidazopyridine-based FASN inhibitor, reduces the number of cells in the S phase by 57% in a highly metastatic OSCC carcinoma cell line LN-1A. The mechanisms by which FASN inhibitors affect the cell cycle progression are not well described. Zadra and Loda (2019) demonstrated that the treatment of prostate cancer cell lines with IPI-9119 reduced the cell cycle kinetics by decreasing the levels of cyclin A2. Other studies have shown that the inhibition of FASN in cancer cell lines may affect several proteins involved in cell cycle control (Agostini et al., 2014, Deepa et al., 2013, Sangeetha et al., 2015, Ventura et al., 2015). (Scaglia, 2014) observed with the incorporation of 14C choline that the levels of fatty acids in cell membranes increase during cell

cycle progression and reached the peak in G2/M. According to the same authors, the presence of a lipogenic checkpoint in the G2/M phase could explain, at least in part, the reduction of the cell cycle progression in FASN-inhibited tumor cells.

We also observed here that the accumulation of SCC-9 cells in G0/G1 and inhibition of S phase was accompanied by apoptosis. Although the treatment with the low concentrations of C75 and ORL promotes cell cycle arrest, apoptotic levels were slightly or not affected. Conversely, IC50 concentration of these drugs significantly increased apoptosis. In fact, TCS was the most effective FASN inhibitor in order to increase apoptosis. TCS was effective even at low concentrations and produced a dose-dependent increase in apoptotic levels. TCS reduces cell growth and viability of tumor cell lines, such as breast cancer (MCF-7 and SKBr-3) end retinoblastoma (Y79) (Deepa et al., 2012, Liu et al., 2002). According to our findings, Sadowski et al. (2014) compared the inhibitory effect of TCS, C75, and ORL in normal and prostate cancer cell lines and found that TCS has a greater cytotoxic effect and the lowest IC50. The biological mechanisms that underlie the cell cycle arrest and apoptosis promoted by the FASN inhibitors need future mechanistic investigation. However, previous studies of our group has shown that FASN activity is necessary for proliferation and survival of OSCC cells considering that both, pharmacological or specific FASN inhibition, reduced the total lipid biosynthesis in OSCC cells (by incorporation studies of 14 C-acetate).

Here we found that while ORL did not affect cell adhesion and invasion and slightly decreases migration of SCC-9 cells, C75 and TCS reduced in more than 50% migration and invasion. In addition, C75 did not significantly affected the adhesion of SCC-9 to type I collagen and fibronectin and TCS promoted a dose-dependent reduction of cell adhesion to the studied extracellular matrix components. The role of FASN in adhesion, migration, and invasion processes are still not clear. Our group has shown that TVB-3166 significantly increases adhesion of SCC-9 and LN-1A cells to myogel, a matrix prepared from human uterine leiomyoma composed mainly by fibronectin, laminin, integrins and different collagens but reduced migration of SCC-9 cells. Zaytseva et al. (2012) showed that FASN inhibition with siRNA in colon cancer cells reduces the levels of MET, Akt, FAK, and paxillin, which are involved in cell adhesion and invasion. (Jafari, 2019) suggested that the inhibition of FASN by TVB-3664 decreases the number of adhesion plaques in primary and metastatic colorectal cancer cells by immunofluorescence reactions for p-FAK and p-paxillin. Recently, (De Piano, 2020)observed that FASN depletion using shRNA increases cell adhesion to matrigel and type I collagen in prostate cancer cell lines (CPTX 1542 and PC3) by increasing the paxillin levels and decreasing the palmitoylation of RhoU. Considering the controversial results in the literature and the different effects of C75, TCS, and ORL it is possible to speculate that cell type and the method used

for the FASN inhibition can modulate the effect on cell adhesion. Despite the promising results in vitro and/or in vivo, is important to emphasize that C75, TCS and ORL are not available for clinical trials of cancer and demonstrated limitations of pharmacological properties and side-effects (Menendez and Lupu, 2017b, Menendez and Lupu, 2017a). In fact, new formulations using nanoparticles would be helpful to improve the drug permeability, absorption and bioavailability of the compounds (Chu et al., 2016).

In summary, we found that C75, TCS, and ORL have distinct effects in the tumorigenic phenotype of SCC-9 cells. C75 has the lowest $IC^{50}$, better inhibition of FASN at low concentrations, and an important reduction of the cell motility phenotypes, especially migration and invasion. TCS has the intermediate $IC_{50}$ and an excellent reduction of lipid bodies at its IC50. TCS also significantly reduces cell cycle progression, adhesion, migration, and invasion while induces high levels of apoptosis in SCC-9 cells. ORL is effective in promoting cell cycle arrest, but induces low levels of apoptosis and did not affect invasion and adhesion. These results indicate that TCS interfere in all the tumorigenic phenotypes of SCC-9 cells.

## CREDIT AUTHORSHIP CONTRIBUTION STATEMENT

Willian Peter Boelcke: Planned and performed experiments, Analyzed data, Wrote and approved the final version of the manuscript. Isadora Ferrari Teixeira: Planned and performed experiments, Analyzed data, Wrote and approved the final version of the manuscript. Iara Gonçalves de Aquino: Performed experiments, Revised and approved the final version of the manuscript. Amanda Mazzaro: Analyzed data, Revised and approved the final version of the manuscript. Florence Juana Maria Cuadra-Zelaya: Analysed data, Revised and approved the final version of the manuscript. Ana Paula Souza: Analyzed data, Revised and approved the final version of the manuscript. Tuula Salo: Analyzed data, Revised and approved the final version of the manuscript. Ricardo Della Coletta: Analyzed data, Discussed the results, Revised and approved the final version of the manuscript. Edgard Graner: Analyzed data, Planned the experiments, Discussed the results, Revised and approved the final version of the manuscript. Débora Campanella Bastos: Conceived, planned and performed experiments, Analyzed data, Wrote, revised and approved the final version of the manuscript.

## ACKNOWLEDGMENTS

This work was supported by the Fundação de Amparo à Pesquisa do Estado de São Paulo - Brazil (FAPESP, 2014/20832-3, 2016/07129-7 and 2016/24906-7) and Coordenação de Aperfeiçoamento de Pessoal de Nível Superior – Brazil (CAPES - 8882.306833/2018–0 and 8887.352647/2019–0).

## REFERENCES

Agostini, M., Almeida, L. Y., Bastos, D. C., Ortega, R. M., Moreira, F. S., Seguin, F., & Graner, E. (2014). The fatty acid synthase inhibitor orlistat reduces the growth and,metastasis of orthotopic tongue oral squamous cell carcinomas. Molecular Cancer Therapeutics, 13(3), 585–595. https://doi.org/10.1158/1535-7163.MCT-12-1136

de Andrade, N. P., Rodrigues, M. F. S. D., Rodini, C. O., & Nunes, F. D. (2017). Cancer stem cell, cytokeratins and epithelial to mesenchymal transition markers expression in oral squamous cell carcinoma derived from ortothopic xenoimplantation of CD44high cells. Pathology Research and Practice, 213(3), 235–244. https://doi.org/10.1016/j.prp.2016.12.009

Angeles, T. S., & Hudkins, R. L. (2016). Recent advances in targeting the fatty acid biosynthetic pathway using fatty acid synthase inhibitors. Expert Opinion on Drug Discovery, 11(12), 1187–1199. https://doi.org/10.1080/17460441.2016.1245286

Aquino, I. G., de, Bastos, D. C., Cuadra-Zelaya, F. J. M., Teixeira, I. F., Salo, T., Coletta, R., ... Graner, E. (2020). Anticancer properties of the fatty acid synthase inhibitor TVB-3166 on oral squamous cell carcinoma cell lines. Archives of Oral Biology, 113(December 2019), Article 104707. https://doi.org/10.1016/j.archoralbio.2020.104707

Bastos, D. C., Paupert, J., Maillard, C., Seguin, F., Carvalho, M. A., Agostini, M., & Graner, E. (2017). Effects of fatty acid synthase inhibitors on lymphatic vessels: an in vitro and in vivo study in a melanoma model. Laboratory Investigation; a Journal of Technical Methods and Pathology, 97(2), 194–206. https://doi.org/10.1038/labinvest.2016.125

Buckley, D., Duke, G., Heuer, T. S., O'Farrell, M., Wagman, A. S., McCulloch, W., & Kemble, G. (2017). Fatty acid synthase - Modern tumor cell biology insights into a classical oncology target. Pharmacology & Therapeutics, 177, 23–31. https://doi.org/10.1016/j.pharmthera.2017.02.021

Carvalho, M. A., Zecchin, K. G., Seguin, F., Bastos, D. C., Agostini, M., Rangel, A. L. C. A., & Graner, E. (2008). Fatty acid synthase inhibition with Orlistat promotes apoptosis and reduces cell

growth and lymph node metastasis in a mouse melanoma model. International Journal of Cancer, 123(11), 2557–2565. https://doi.org/10.1002/ijc.23835

Chen, M., Huang, J., Yang, X., Liu, B., Zhang, W., Huang, L., & Ge, J. (2012). Serum starvation induced cell cycle synchronization facilitates human somatic cells reprogramming. PLoS ONE, 7(4). https://doi.org/10.1371/journal.pone.0028203

Chen, P., Li, L., Wang, H., Zhao, J., Cheng, Y., Xie, J., & Gong, S. (2020). Omeprazole, an inhibitor of proton pump, suppresses De novo lipogenesis in gastric epithelial cells. Biomedicine and Pharmacotherapy, 130(June), Article 110472. https://doi.org/10.1016/j.biopha.2020.110472

Chu, C., Deng, J., Liu, L., Cao, Y., Wei, X., Li, J., & Man, Y. (2016). Nanoparticles combined with growth factors: Recent progress and applications. RSC Advances, 6 (93), 90856–90872. https://doi.org/10.1039/c6ra13636b

Chu, C., Deng, J., Man, Y., & Qu, Y. (2017). Green tea extracts epigallocatechin-3-gallate for different treatments. BioMed Research International, 2017. https://doi.org/10.1155/2017/5615647

Cohen Goldemberg, D., de Araújo, L. H. L., Antunes, H. S., de Melo, A. C., & Santos Thuler, L. C. (2018). Tongue cancer epidemiology in Brazil: incidence, morbidity and mortality. Head and Neck, 40(8), 1834–1844. https://doi.org/10.1002/hed.25166

De Piano, Mario, et al. (2020). Lipogenic signalling modulates prostate cancer cell adhesion and migration via modification of Rho GTPases. Oncogene, 38(18), 3666–3679. https://doi.org/10.1038/s41388-020-1243-2

Deepa, P. R., Vandhana, S., Jayanthi, U., & Krishnakumar, S. (2012). Therapeutic and Toxicologic Evaluation of Anti-Lipogenic Agents in Cancer Cells Compared with Non-Neoplastic Cells. Basic and Clinical. Pharmacology and Toxicology, 110(6),494–503. https://doi.org/10.1111/j.1742-7843.2011.00844.x

Deepa, P. R., Vandhana, S., & Krishnakumar, S. (2013). Fatty acid synthase inhibition induces differential expression of genes involved in apoptosis and cell proliferation in ocular cancer cells. Nutrition and Cancer, 65(2), 311–316. https://doi.org/10.1080/01635581.2013.748923

Gir´o-Perafita, A., Palomeras, S., Lum, D. H., Blancafort, A., Vi˜nas, G., Oliveras, G., & uig, T. (2016). Preclinical evaluation of fatty acid synthase and egfrinhibition in triple-negative breast cancer. Clinical Cancer Research, 22(18), 4687–4697. https://doi.org/10.1158/1078-0432.CCR-15-3133

Hanahan, D., & Weinberg, R. A. (2011). Hallmarks of cancer: The next generation. Cell, 144(5), 646–674. https://doi.org/10.1016/j.cell.2011.02.013

Heuer, T. S., Ventura, R., Mordec, K., Lai, J., Fridlib, M., Buckley, D., & Kemble, G. (2017). FASN inhibition and taxane treatment combine to enhance anti-tumor efficacy in diverse xenograft tumor models through disruption of tubulin palmitoylation and microtubule organization and FASN inhibition-mediated effects

on oncogenic signaling and gene ex. EBioMedicine, 16, 51–62. https://doi.org/ 0.1016/j.ebiom.2016.12.012

Ho, A. S., Kim, S., Tighiouart, M., Gudino, C., Mita, A., Scher, K. S., & Zumsteg, Z. S. (2017). Metastatic lymph node burden and survival in oral cavity cancer. Journal of Clinical Oncology, 35(31), 3601–3609. https://doi.org/10.1200/JCO.2016.71.1176

Jafari. (2019). De Novo Fatty Acid Synthesis-Driven Sphingolipid Metabolism Promotes Metastatic Potential of Colorectal Cancer. Molecular Cancer Research, 17(1), 140–152. https://doi.org/10.1158/1541-7786.MCR-18-0199

Jones, S. F., & Infante, J. R. (2015). Molecular pathways: fatty acid synthase. ClinicalCancer Research: An Official Journal of the American Association for Cancer Research,21(24), 5434–5438. https://doi.org/10.1158/1078-0432.CCR-15-0126

Kelber, J. A., Cao, H. S. T., Cantin, G. T., Lin, R., Wang, W., Kaushal, S., & Yates, J. R. (2010). Correction for Chiaroni et al., Y chromosome diversity, human expansion, drift, and cultural evolution. Proceedings of the National Academy of Sciences, 107(30). https://doi.org/10.1073/pnas.1008738107, 13556-13556.

Kridel, S. J., Axelrod, F., Rozenkrantz, N., & Smith, J. W. (2004). Orlistat is a novel inhibitor of fatty acid synthase with antitumor activity. Cancer Research, 64(6), 2070–2075. Retrieved from http://www.ncbi.nlm.nih.gov/pubmed/15026345.

Kuhajda, F. P. (2000). Fatty-acid synthase and human cancer: New perspectives on its,role in tumor biology. Nutrition, 16(3), 202–208. https://doi.org/10.1016/S0899-9007(99)00266-X

Liu, B., Wang, Y., Fillgrove, K. L., & Anderson, V. E. (2002). Triclosan inhibits enoyl-reductase of type I fatty acid synthase in vitro and is cytotoxic to MCF-7 and SKBr-3 breast cancer cells. Cancer Chemotherapy and Pharmacology, 49(3), 187–193. https://doi.org/10.1007/s00280-001-0399-x

Liu, Y. (2006). Fatty acid oxidation is a dominant bioenergetic pathway in prostate cancer. Prostate Cancer and Prostatic Diseases, 9(3), 230–234. https://doi.org/10.1038/sj.pcan.4500879

Lupu, R., & Menendez, J. A. (2006). Pharmacological inhibitors of Fatty Acid Synthase (FASN)–catalyzed endogenous fatty acid biogenesis: a new family of anti-cancer agents? Current Pharmaceutical Biotechnology, 7(6), 483–493. Retrieved from 〈 http://www.ncbi.nlm.nih.gov/pubmed/17168665〉.

Mendonça, B. D. S., Agostini, M., Aquino, I. G., Dias, W. B., Bastos, D. C., & Rumjanek, F. D. (2017). Suppression of MAGE-A10 alters the metastatic phenotype of tongue squamous cell carcinoma cells. Biochemistry and Biophysics Reports, 10, 267–275. https://doi.org/10.1016/j.bbrep.2017.04.009

Menendez, J. A., & Lupu, R. (2017a). Fatty acid synthase regulates estrogen receptor-α signaling in breast cancer cells. e299-11 Oncogenesis, 6(2). https://doi.org/10.1038/ oncsis.2017.4.

Menendez, J. A., & Lupu, R. (2017b). Fatty acid synthase (FASN) as a therapeutic target in breast cancer. Expert Opinion on Therapeutic Targets, 21(11), 1001–1016. https://doi.org/10.1080/14728222.2017.1381087

Menendez, J. A., Vellon, L., Espinoza, I., & Lupu, R. (2016). The metastasis inducer CCN1 (CYR61) activates the fatty acid synthase (FASN)-driven lipogenic phenotype in breast cancer cells. Oncoscience, 3(7–8), 242–257. https://doi.org/10.18632/oncoscience.314

Menendez, J. A., Vellon, L., Mehmi, I., Oza, B. P., Ropero, S., Colomer, R., & Lupu, R. (2004). Inhibition of fatty acid synthase (FAS) suppresses HER2/neu (erbB-2) oncogene overexpression in cancer cells. Proceedings of the National Academy of Sciences of the United States of America, 101(29), 10715–10720. https://doi.org/10.1073/pnas.0403390101

Montero, P. H., & Patel, S. G. (2015). Cancer of the oral cavity. Surgical Oncology Clinics of North America, 24(3), 491–508. https://doi.org/10.1016/j.soc.2015.03.006

Oslob, J. D., Johnson, R. J., Cai, H., Feng, S. Q., Hu, L., Kosaka, Y., & McDowell, R. S. (2013). Imidazopyridine-based fatty acid synthase inhibitors that show anti-HCV activity and in vivo target modulation. ACS Medicinal Chemistry Letters, 4(1),113–117. https://doi.org/10.1021/ml300335r

Puig, T., V´azquez-Martín, A., Relat, J., P´etriz, J., Men´endez, J. A., Porta, R., & Colomer, R. (2008). Fatty acid metabolism in breast cancer cells: differential inhibitory effects of epigallocatechin gallate

(EGCG) and C75. Breast Cancer Research and Treatment, 109(3), 471–479. https://doi.org/10.1007/s10549-007-9678-5

Ramos, D. M., But, M., Regezi, J., Schmidt, B. L., Atakilit, A., Dang, D., & Li, X. (2002). Expression of integrin β6 enhances invasive behavior in oral squamous cell carcinoma. Matrix Biology, 21(3), 297–307. https://doi.org/10.1016/S0945-053X (02)00002-1

Relat, J., Blancafort, A., Oliveras, G., Cufí, S., Haro, D., Marrero, P. F., & Puig, T. (2012). Different fatty acid metabolism effects of (-)-epigallocatechin-3-gallate and C75 in adenocarcinoma lung cancer. BMC Cancer, 12, 280. https://doi.org/10.1186/1471-2407-12-280

Rendina, A. R., & Cheng, D. (2005). Characterization of the inactivation of rat fatty acid synthase by C75: Inhibition of partial reactions and protection by substrates. Biochemical Journal, 388(3), 895–903. https://doi.org/10.1042/BJ20041963

Rheinwald, J. G., & Beckett, M. A. (1981). Tumorigenic keratinocyte lines requiring anchorage and fibroblast support cultured from human squamous cell carcinomas. Cancer Research, 41(5), 1657–1663.

Ricklefs, F. L., Maire, C. L., Matschke, J., Dührsen, L., Sauvigny, T., Holz, M., & Lamszus, K. (2020). Fasn is a biomarker enriched in malignant glioma-derived extracellular vesicles. International Journal of Molecular Sciences, 21(6). https://doi.org/10.3390/ijms21061931

R¨ohrig, F., & Schulze, A. (2016). The multifaceted roles of fatty acid synthesis in cancer. Nature Reviews Cancer, 16(11), 732–749. https://doi.org/10.1038/nrc.2016.89

Sadowski, M. C., Pouwer, R. H., Gunter, J. H., Lubik, A. A., Quinn, R. J., & Nelson, C. C. (2014). The fatty acid synthase inhibitor triclosan: repurposing an anti-microbial agent for targeting prostate cancer. Oncotarget, 5(19), 9362–9381. https://doi.org/10.18632/oncotarget.2433

Salo, T., Sutinen, M., Hoque Apu, E., Sundquist, E., Cervigne, N. K., de Oliveira, C. E., & Coletta, R. D. (2015). A novel human leiomyoma tissue derived matrix for cell culture studies. BMC Cancer, 15(1), 1. https://doi.org/10.1186/s12885-015-1944-z

Sangeetha, M., Deepa, P. R., Rishi, P., Khetan, V., & Krishnakumar, S. (2015). Global Gene Deregulations in FASN Silenced Retinoblastoma Cancer Cells: Molecular and Clinico-Pathological Correlations. Journal of Cellular Biochemistry, 116(11), 2676–2694. https://doi.org/10.1002/jcb.25217

Sardesai, S. D., Thomas, A., Gallagher, C., Lynce, F., Ottaviano, Y. L., Ballinger, T. J., & Miller, K. D. (2021). Inhibiting Fatty Acid Synthase with Omeprazole to Improve Efficacy of Neoadjuvant Chemotherapy in Patients with Operable TNBC. Clinical Cancer Research: An Official Journal of the American Association for Cancer Research, 27(21), 5810–5817. https://doi.org/10.1158/1078-0432.CCR-21-0493

Scaglia, Natalia (2014). De novo fatty acid synthesis at the mitotic exit is required to complete cellular division. Cell Cycle, 13(5), 859–868. https://doi.org/10.4161/cc.27767

Seguin, F., Carvalho, M. A., Bastos, D. C., Agostini, M., Zecchin, K. G., Alvarez-Flores, M. P., & Graner, E. (2012). The fatty acid synthase inhibitor orlistat reduces experimental metastases and angiogenesis in B16-F10 melanomas. British Journal of Cancer, 107(6). https://doi.org/10.1038/bjc.2012.355

Silva, S. D., Cunha, I. W., Younes, R. N., Soares, F. A., Kowalski, L. P., & Graner, E. (2010). ErbB receptors and fatty acid synthase expression in aggressive head and neck squamous cell carcinomas. Oral Diseases, 16(8), 774–780. https://doi.org/10.1111/j.1601-0825.2010.01687.x

Silva, S. D., Perez, D. E., Nishimoto, I. N., Alves, F. A., Pinto, C. A. L., Kowalski, L. P., & Graner, E. (2008). Fatty acid synthase expression in squamous cell carcinoma of the tongue: clinicopathological findings. Oral Diseases, 14(4), 376–382. https://doi.org/10.1111/j.1601-0825.2007.01395.x

Silva, S. D. D., Cunha, I. W., Nishimoto, I. N., Soares, F. A., Carraro, D. M., Kowalski, L. P., & Graner, E. (2009). Clinicopathological significance of ubiquitin-specific protease 2a (USP2a), fatty acid synthase (FASN), and ErbB2 expression in oral squamous cell carcinomas. Oral Oncology, 45(10), e134–e139. https://doi.org/10.1016/j.oraloncology.2009.02.004

Sippel, K. H., Vyas, N. K., Zhang, W., Sankaran, B., & Quiocho, F. A. (2014). Crystal structure of the human fatty acid synthase enoyl-acyl carrier protein-reductase domain complexed with triclosan reveals allosteric protein-protein interface inhibition. Journal of Biological Chemistry, 289(48), 33287–33295. https://doi.org/10.1074/jbc.M114.608547

Smith, S., Witkowski, A., & Joshi, A. K. (2003). Structural and functional organization of the animal fatty acid synthase. Progress in Lipid Research, 42(4), 289–317 (Retrieved from) 〈 http://www.ncbi.nlm.nih.gov/pubmed/12689621〉.

Vandhana, S., Coral, K., Jayanthi, U., Deepa, P. R., & Krishnakumar, S. (2013). Biochemical changes accompanying apoptotic cell death in retinoblastoma cancer cells treated with lipogenic enzyme inhibitors. Biochimica et Biophysica Acta -Molecular and Cell Biology of Lipids, 1831(9), 1458–1466. https://doi.org/10.1016/j.bbalip.2013.06.005

Veigel, D., Wagner, R., Stübiger, G., Wuczkowski, M., Filipits, M., Horvat, R., & Grunt, T. W. (2015). Fatty acid synthase is a metabolic marker of cell proliferation rather than malignancy in ovarian cancer and its precursor cells. International Journal of Cancer, 136(9), 2078–2090. https://doi.org/10.1002/ijc.29261

Ventura, R., Mordec, K., Waszczuk, J., Wang, Z., Lai, J., Fridlib, M., & Heuer, T. S. (2015). Inhibition of de novo Palmitate Synthesis by Fatty Acid Synthase Induces Apoptosis in Tumor Cells by Remodeling Cell Membranes, Inhibiting Signaling Pathways, and Reprogramming Gene Expression. EBioMedicine, 2(8), 808–824. https://doi.org/10.1016/j.ebiom.2015.06.020

Wang, X., Lin, J., Chen, Y., Zhong, W., Zhao, G., Liu, H., & Li, S. (2009). Novel fatty acid synthase (FAS) inhibitors: Design, synthesis, biological evaluation, and molecular docking studies. Bioorganic and Medicinal Chemistry, 17(5), 1898–1904. https://doi.org/10.1016/j.bmc.2009.01.050

Witkiewicz, A. K., Nguyen, K. H., Dasgupta, A., Kennedy, E. P., Yeo, C. J., Lisanti, M. P., & Brody, J. R. (2008). Co-expression of fatty acid synthase and caveolin-1 in pancreatic ductal adenocarcinoma: Implications for tumor progression and clinical outcome. Cell Cycle, 7(19), 3021–3025. https://doi.org/10.4161/cc.7.19.6719

Zadra, G., & Loda, M. (2019). When fat goes down, prostate cancer is on the ropes. Molecular and Cellular Oncology, 6(3), 1–3. https://doi.org/10.1080/23723556.2019.1595308

Zadra, Giorgia (2019). Inhibition of de novo lipogenesis targets androgen receptor signaling in castration-resistant prostate cancer. PNAS, 116(2), 631–640. https://doi.org/10.1073/pnas.1808834116

Zaytseva, Y. Y., Rychahou, P. G., Gulhati, P., Elliott, V. A., Mustain, W. C., O'Connor, K., & Evers, B. M. (2012). Inhibition of fatty acid synthase attenuates CD44-associated signaling and reduces metastasis in colorectal cancer. Cancer Research, 72(6), 1504–1517. https://doi.org/10.1158/0008-5472.CAN-11-4057

## TABLES

Table 1. IC50 for each drug calculated using dose-response curves with MTT assays.

| FASN inhibitor | $IC_{50}$ 24 h (μM) | $IC_{50}$ 48 h (μM) |
|---|---|---|
| C75 | 26.38 | 11.58 |
| TCS | 37.82 | 23.29 |
| ORL | 294.76 | 138.55 |

FASN: fatty acid synthase; TCS: Triclosan; ORL: Orlistat; IC50: half maximal inhibitory concentration

## FIGURE LEGENDS

**Fig. 1.** FASN inhibition with C75, TCS, and ORL reduces proliferation and induces distinct morphologic changes in SCC-9 cells. The IC50 was calculated using MTT viability assays after treating SCC-9 cells with FASN inhibitors for 24 h (A-C) and 48 h (D-F). C75 (A and D), TCS (B and E) and ORL (C and F) induced a dose-dependent SCC-9 cell death, allowing the determination of IC50. Compared to control cells (G), treatment with the IC50 of C75 (H) induced cytoplasmic retraction (arrow) and predominantly polygonal cells with abundant cytoplasm (arrow). (I) TCS reduced the cell size and increased the number of rounded cells (arrow) and the amount of cytoplasmic granules (arrow). ORL (J) induced a spindle pattern in SCC-9 cells (arrow). Highlighted rounded cells, characteristics of dead cells (arrowheads). Error bar = mean ± SD of at least 3 independent experiments. * $p < 0.05$ ANOVA and Tukey tests. Original 200X magnification.

**Fig. 2.** C75, TCS, and ORL reduces the amount of lipid bodies in SCC-9 cells. Compared with the control cells (A, F and K), the treatment with C75 (B-D), TCS (F-I) and ORL (L-N) significantly reduce the number of lipid bodies normalized by the cell area in comparison with to control cells. (E,J and O) number of lipid droplets stained by bodipy were normalized by the area of each cell. Error bars = mean ± SD of at least 50 cells in 10 microscopic fields (original magnification 400X). # different from all, * $p < 0.05$, ** $p < 0.0001$ ANOVA and Tukey tests (ORL) and Kruskall-Wallis (C75 and TCS).

**Fig. 3**. FASN inhibition promotes cell cycle arrest in G0/G1 and increases the S phase in SCC-9 cells. Treatment of SCC-9 cells with $IC_{12.5}$, $IC_{25}$, and $IC_{50}$ for 48 h of C75 (A) and ORL (C) induces a cell cycle arrest in the G0/G1 phase and reduces the number of cells in the S phase in a dose dependent manner. The treatment of SCC-9 cells with TCS (B) reduces S phase and increases the percentage of cells in the G0/G1at the $IC_{25}$ and $IC_{50}$. The compounds equally affected the S-phase progression at the $IC_{12.5}$ (D) but atthe $IC_{25}$ (E) and $IC_{50}$ (F), TCS and ORL show higher inhibitory effect onS-phase, when compared to the C75. Error bars = mean ± SD of the experimental triplicate. * $p < 0.05$, ANOVA and Tukey tests.

**Fig. 4**. Apoptosis is induced by FASN inhibitors. The treatment of SCC-9 with the $IC_{50}$ of C75 (A) and the $IC_{25}$ and $IC_{50}$ of TCS (B) reduces the number of viable cells and increases apoptotic cells. All tested concentrations of ORL (C) increase the number of apoptotic cells. TCS was the most effective when compared with C75 and ORL in order to reduce the number of living cells (D) and induce apoptosis (E). Error bar = mean ± SD of the experimental triplicate. * $p < 0.05$, ** $p < 0.005$, *** $p < 0.0001$, ANOVA and Tukey tests.

**Fig. 5**. Cell adhesion is differently modulated by pharmacological FASN inhibitors. The treatment with C75 (A) resulted in a slight increase, not statistically significant, in SCC-9 adhesion at the IC12.5 and IC50. TCS significantly reduces SCC-9 adhesion to fibronectin and type I collagen in all the analyzed concentrations (B) and ORL (C) did not significantly affect the adhesion. Error bar = mean ± SD of the experimental triplicate. # different from all, * $p < 0.05$, ANOVA and Tukey tests.

**Fig. 6**. Migration and invasion phenotypes of SCC-9 cells are affected by the inhibition of FASN. Transwell migration (A-E) and invasion (F-J) assays with SCC-9 cells treated with the $IC_{50}$ of C75, TCS and ORL. C75 (B) and TCS (C) showed a significant inhibition (E) of cell migration when compared to the control (A) and to the ORL (D). The invasiveness of the cells were significantly affected by C75 (G) and TCS (H) but not modulated by ORL (I-J). Original magnification 5X. Error bar = mean ± SD of the experimental triplicate. ANOVA and Tukey tests, # different from all, * $p < 0.05$, ** $p < 0.005$.

## FIGURES

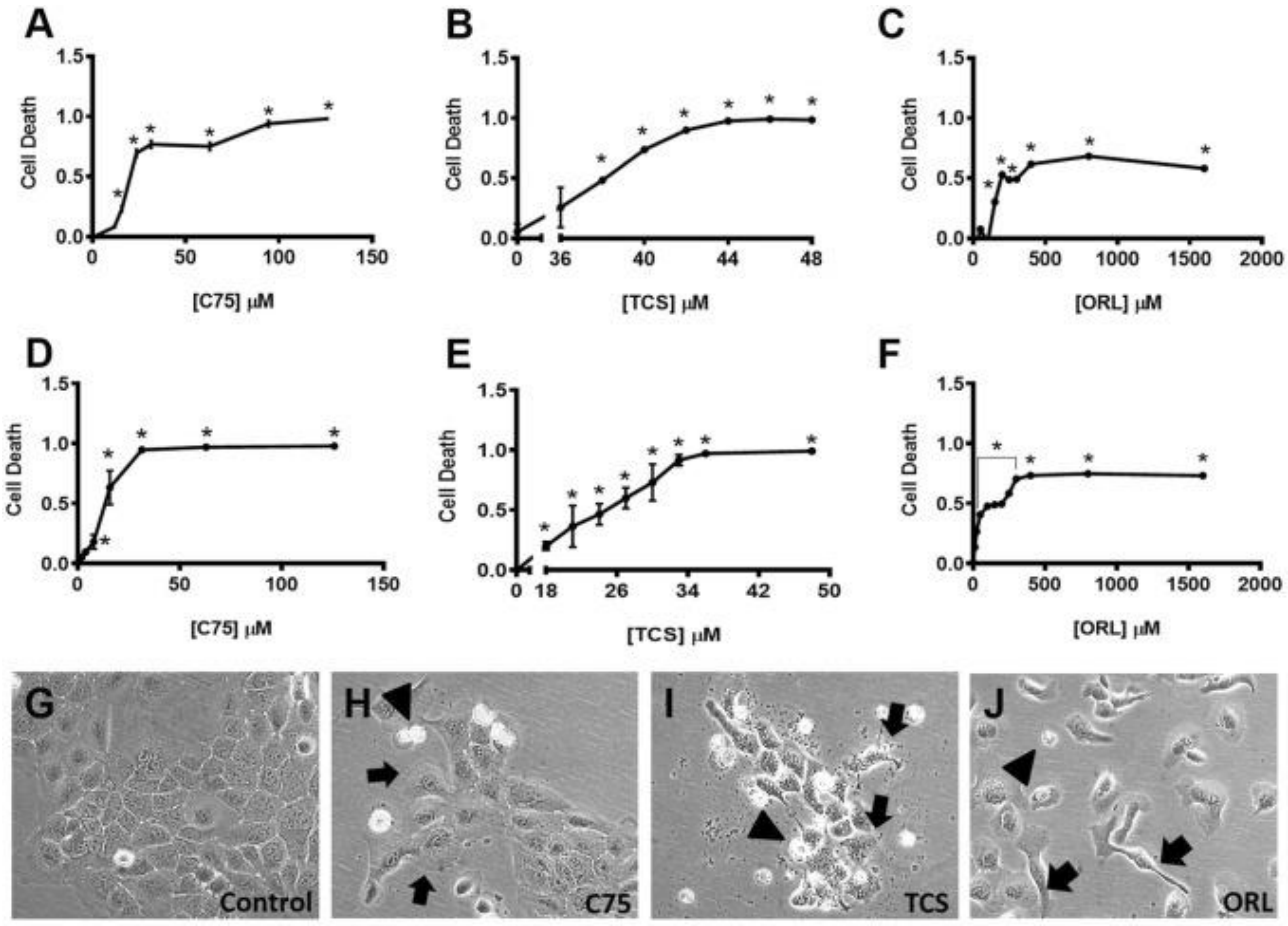
A
B
C
D
E
F
Cell Death
[C75] μM
[TCS] μM
[ORL] μM
G
H
I
J
Control
C75
TCS
ORL

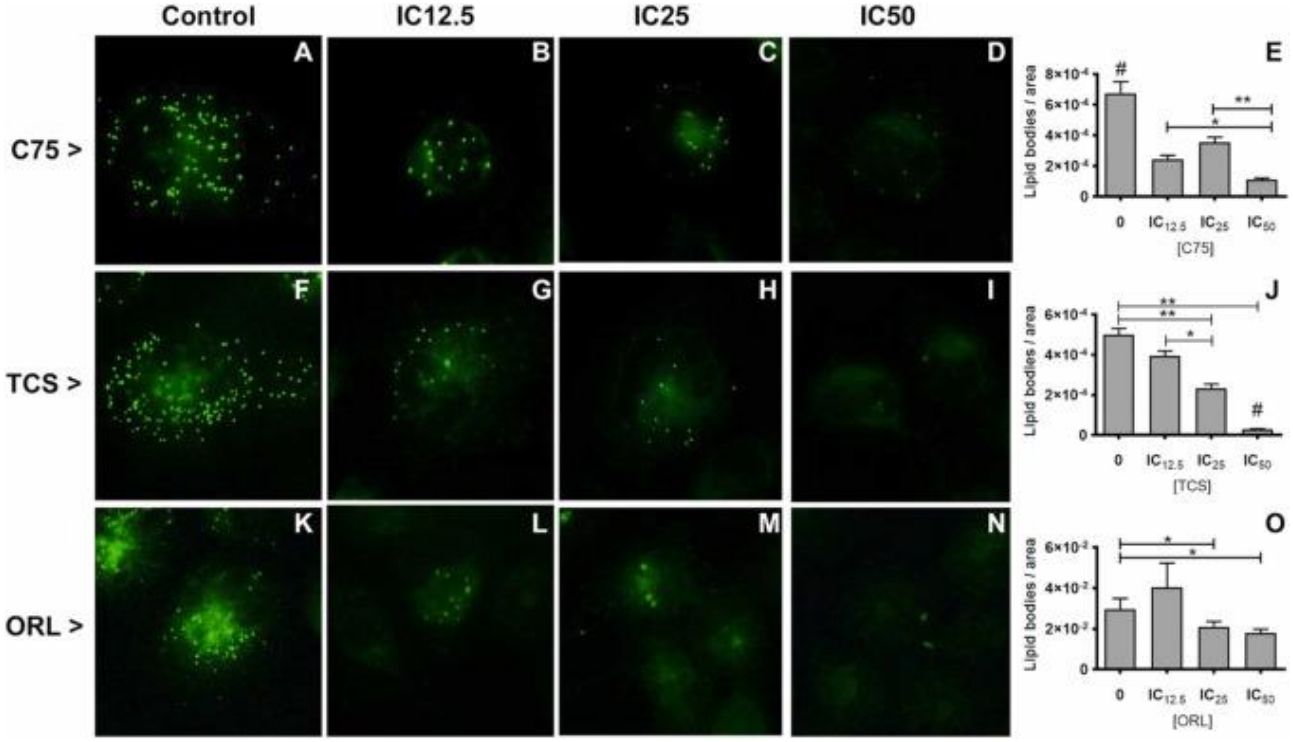
Control
IC12.5
IC25
IC50
C75 >
TCS >
ORL >
A
B
C
D
E
F
G
H
I
J
K
L
M
N
O
Lipid bodies / area
0
IC12.5
IC25
IC50
[C75]
[TCS]
[ORL]

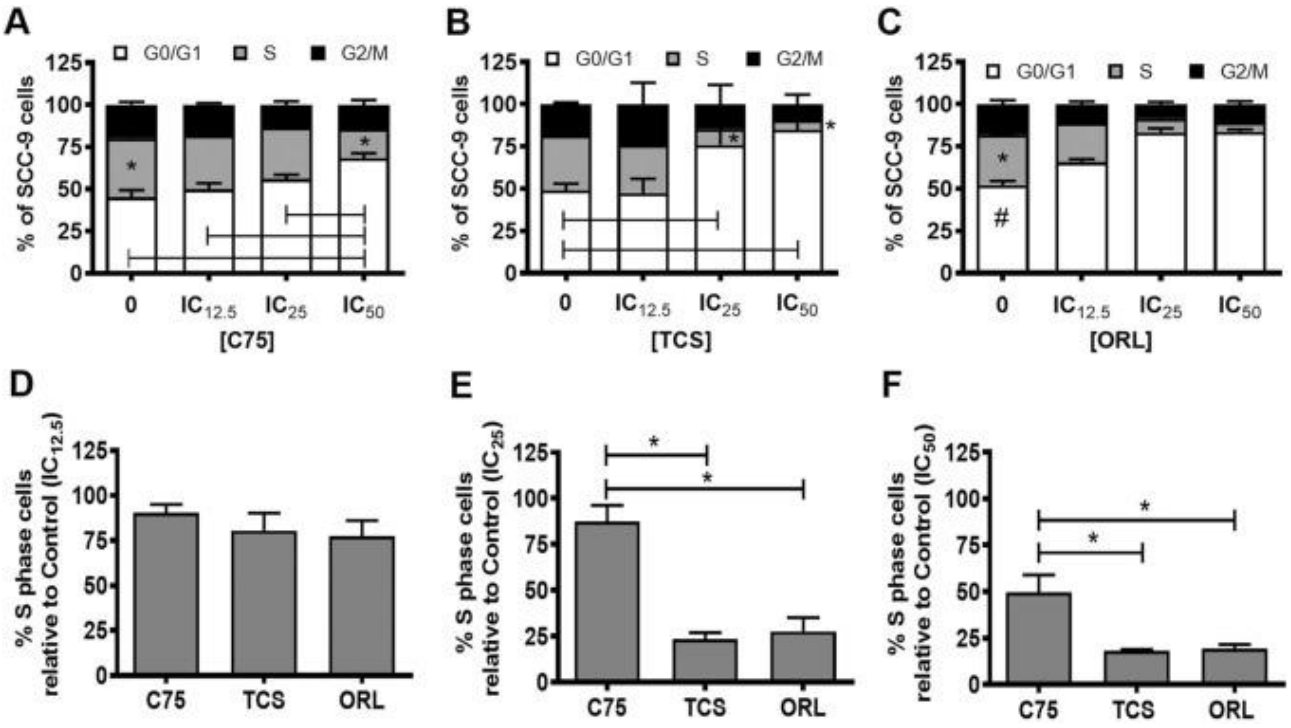
A
B
C
G0/G1
S
G2/M
% of SCC-9 cells
0
IC12.5
IC25
IC50
[C75]
[TCS]
[ORL]
D
E
F
% S phase cells relative to Control (IC12.5)
% S phase cells relative to Control (IC25)
% S phase cells relative to Control (IC50)
C75
TCS
ORL

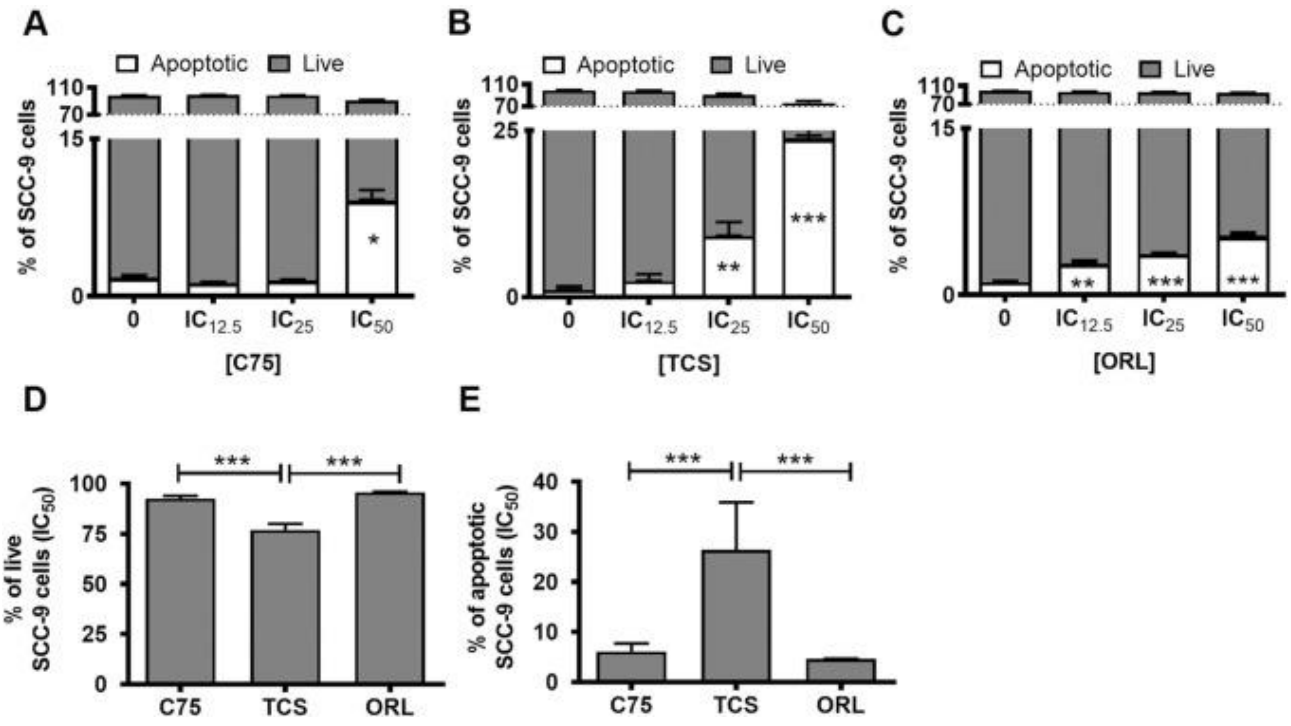
A
Apoptotic
Live
% of SCC-9 cells
110
70
15
0
*
0
IC12.5
IC25
IC50
[C75]
B
Apoptotic
Live
% of SCC-9 cells
110
70
25
0
**
***
0
IC12.5
IC25
IC50
[TCS]
C
Apoptotic
Live
% of SCC-9 cells
110
70
15
0
**
***
***
0
IC12.5
IC25
IC50
[ORL]
D
% of live SCC-9 cells (IC50)
***
***
100
75
50
25
0
C75
TCS
ORL
E
% of apoptotic SCC-9 cells (IC50)
***
***
40
30
20
10
0
C75
TCS
ORL

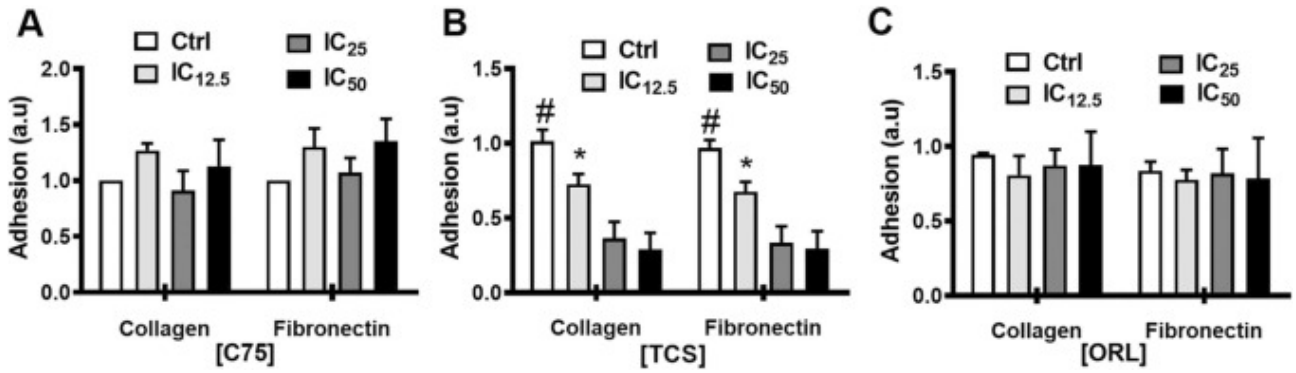
A
Ctrl
IC12.5
IC25
IC50
Adhesion (a.u)
2.0
1.5
1.0
0.5
0.0
Collagen
Fibronectin
[C75]
B
Ctrl
IC12.5
IC25
IC50
#
*
#
*
Adhesion (a.u)
1.5
1.0
0.5
0.0
Collagen
Fibronectin
[TCS]
C
Ctrl
IC12.5
IC25
IC50
Adhesion (a.u)
1.5
1.0
0.5
0.0
Collagen
Fibronectin
[ORL]

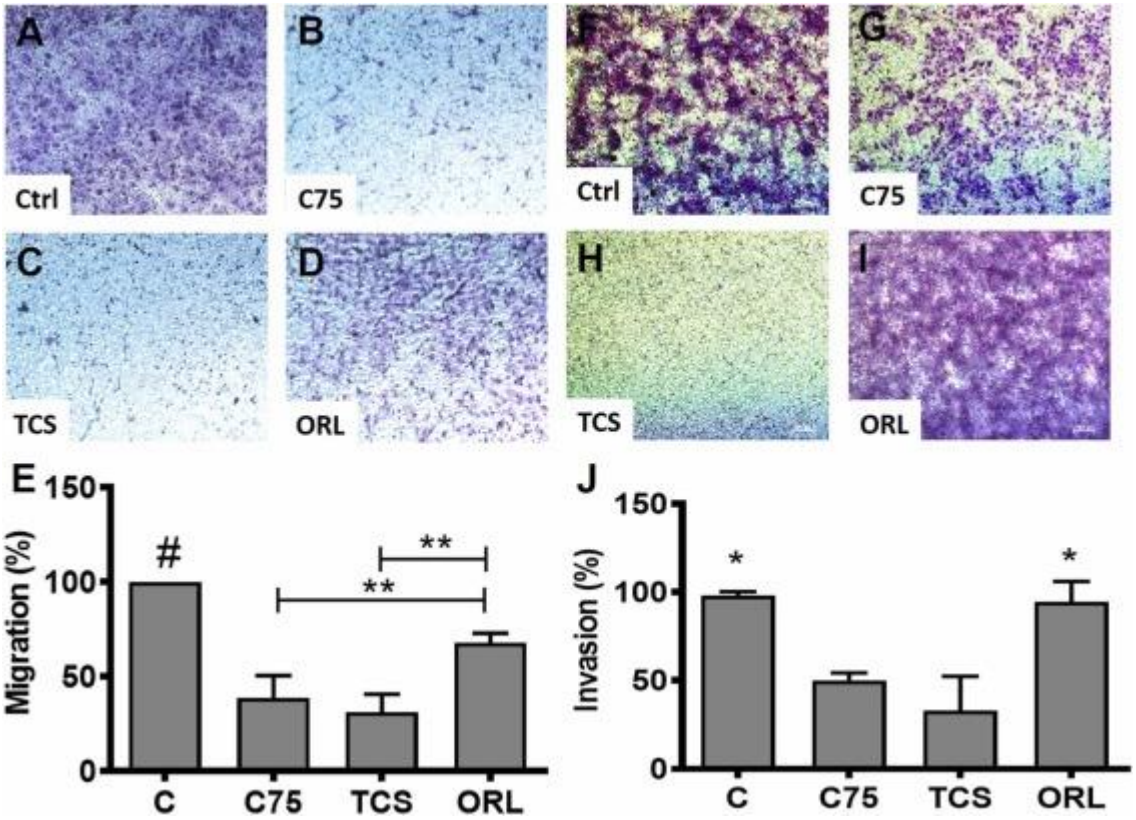
A
Ctrl
B
C75
F
Ctrl
G
C75
C
TCS
D
ORL
H
TCS
I
ORL
E
Migration (%)
150
100
50
0
#
**
**
C
C75
TCS
ORL
J
Invasion (%)
150
100
50
0
*
*
C
C75
TCS
ORL